Articles

Contribution from the Central Research and Development Department,
E. I. du Pont de Nemours and Company, Experimental Station, Wilmington, Delaware 19898

Pyridinium Molybdates. Synthesis and Structure of an Octamolybdate Containing Coordinately Bound Pyridine: [(C5H5N)2Mo8O26]4−

E. M. McCARRON, III,* J. F. WHITNEY, and D. B. CHASE

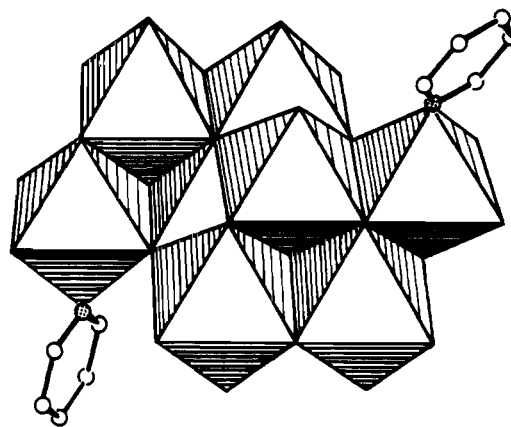Molybdenum trioxide dihydrate reacts with pyridine to give the octamolybdates $(C_5H_5NH)_4[Mo_8O_{26}]$ (1) and $(C_5H_5NH)_4[(C_5H_5N)_2Mo_8O_{26}]$ (2). Recrystallization of 2 in a 2:1 mixture of dimethyl sulfoxide and pyridine gives single crystals of $(C_5H_5NH)_4[(C_5H_5N)_2Mo_8O_{26}]\cdot2Me_2SO$. This compound crystallizes with monoclinic symmetry in the space group $P2_1/n$, the cell parameters being $a = 11.388$ Å, $b = 13.761$ Å, $c = 17.547$ Å, $\beta = 100.70°$, $V = 2702$ Å^3, and $Z = 4$. The structure has been solved by MULTAN direct methods and refined to $R = 0.0379$, from 4937 independent reflections. The anion $[(C_5H_5N)_2Mo_8O_{26}]^{4-}$, is built of two $C_5H_5NMoO_5$ and six MoO_6 edge-sharing octahedra, all of which exhibit the typical $2 + 2 + 2$ octahedral distortion. A formation mechanism based on this bond length criterion is proposed. The $Mo-NC_5H_5$ bond length is 2.279 Å, giving a bond strength of $\sim^1/_3$. This weak Mo–N bond is consistent with what is observed for other interactions between Mo(VI) and neutral-base ligands.

Introduction

The recent expansion of the field of isopolymolybdate chemistry to include coordination chemistry, as illustrated by the anions $[Mo_8O_{24}(OCH_3)_4]^{4-}$,[1] $[(HCO)_2Mo_8O_{28}]^{6-}$,[2] and $[CH_2Mo_4O_{15}H]^{3-}$ [3] is of great importance in developing an understanding of how small organic molecules interact with catalytic oxide surfaces.[1,2,4] In each of the three examples cited above, molybdenum interacts with oxygen-donating ligands in such a way that each individual molybdenum atom is octahedrally[5] coordinated to six oxygen atoms. However, on the basis of an analogy with the earlier report[6] of the formation of $(C_5H_5N)MoO_3$ (in which the molybdenum atoms are octahedrally coordinated as follows, $[(C_5H_5N)_{1/1}MoO_{1/1}O_{4/2}]$), it seemed probable that isopolymolybdates containing nitrogen-donating ligands ought to exist. We report here the first example of an isopolymolybdate containing a ligand bound to molybdenum through a donor other than oxygen, namely $[(C_5H_5N)_2Mo_8O_{26}]^{4-}$.

Experimental Section

Preparation of $(C_5H_5NH)_4[Mo_8O_{26}]$. Molybdenum trioxide dihydrate[7] (3.0 g) was heated at 60 °C in an excess of pyridine (150 mL) for 72 h. The resulting white powder was filtered, washed with acetone, and dried at 50 °C under vacuum. Anal. Calcd for $(C_5H_5NH)_4[Mo_8O_{26}]$: C, 16.0; H, 1.6; N, 3.7; MoO_3, 76.6. Found: C, 16.3, H, 1.6; N, 3.9; MoO_3, 77.0.

Preparation of $(C_5H_5NH)[(C_5H_5N)_2Mo_8O_{26}]$. This compound was prepared as above, except that the reaction was carried out at 45 °C for 24 h. Anal. Calcd for $(C_5H_5NH)_4[(C_5H_5N)_2Mo_8O_{26}]$: C, 21.7;

(1) McCarron, E. M., III; Harlow, R. L. *J. Am. Chem. Soc.* **1983**, *105*, 6179.
(2) Adams, R. D.; Klemperer, W. G.; Liu, R.-S. *J. Chem. Soc., Chem. Commun.* **1979**, 256.
(3) Day, V. W.; Fredrich, M. F.; Klemperer, W. G.; Liu, R.-S. *J. Am. Chem. Soc.* **1979**, *101*, 491.
(4) McCarron, E. M., III; Staley, R. H.; Sleight, A. W. *Inorg. Chem.* **1984**, *23*, 1043.
(5) The molybdenum sites exhibit the typical $2 + 2 + 2$ octahedral distortion found in MoO_3: Kihlborg, L. *Ark. Kemi* **1963**, *21*, 357. For a discussion of this molybdenum coordination see: Goodenough, J. B. "Proceedings of the Climax 4th International Conference on the Chemistry and Uses of Molybdenum"; Barry, H. F., Mitchell, P. C. H., Eds.; Climax Molybdenum Co.: Ann Arbor, MI, 1982.
(6) Johnson, J. W.; Jacobson, A. J.; Rich S. M.; Brody, J. F. *J. Am. Chem. Soc.* **1981**, *103*, 5246; *Rev. Chim. Miner.* **1982**, *19*, 420.

(7) "Handbook of Preparative Inorganic Chemistry", 2nd ed.; Brauer, G. Ed.; Academic Press: New York, 1965; p 1412.

H, 2.1; N, 5.1; MoO_3, 69.3. Found: C, 21.7; H, 2.1; N, 5.2; MoO_3, 70.0.

The interaction of the $[(C_5H_5N)_2Mo_8O_{26}]^{4-}$ anion with water results in the loss of pyridine (as determined by its distinctive odor and later confirmed by mass spectrometry) to give the simple molybdate $(C_5H_5NH)_4[Mo_8O_{26}]$.

Preparation of $(C_5H_5NH)_4[(C_5H_5N)_2Mo_8O_{26}]\cdot2Me_2SO$. $(C_5H_5NH)_4[(C_5H_5N)_2Mo_8O_{26}]$, prepared as described above, was recrystallized from a 2:1 mixture, by volume, of dimethyl sulfoxide and pyridine. Colorless parallelepiped crystals were observed to form after ~24 h at room temperature. A typical crystal measured ~0.25 × 0.20 × 0.30 mm. A suitable crystal was selected and used in the structure determination.

Spectroscopic Studies. The infrared spectra were recorded in diffuse reflectance of both neat powders and diluted samples (4:1 with KBr) using a Nicolet 7199 interferometer with a diffuse reflectance bench. A total of 256 scans were coadded at 1-cm^{-1} spectral resolution, and a polynomial apodization function was employed. Fine powdered KBr was used as a reflectance standard. The spectra showed no major differences between dilute and pure samples, ensuring that no anomalous specular reflection features were being observed.

Raman spectra were recorded with a J-Y microprobe operating in the microscopic mode. Radiation of 5145 Å was used with an incident power level of 10–20 mW at the sample. The spectral slit width was 2 cm^{-1}, and step scan data acquisition (step size 1 cm^{-1}) was employed. Spectra taken at various power levels showed no evidence of photochemical or thermal degradation.

Decomposition Studies. Thermogravimetric analyses were carried out on a Du Pont 951-990 instrument at a heating rate of 5 °C/min both in oxygen and under vacuum. Analyses of thermal decomposition products were performed on a Du Pont 21-491 gas chromatography/mass spectrometry instrument. Powdered samples were loaded into a 120 Pyroprobe unit under a flowing He stream and flashed (20°/ms) to the desired temperatures.

X-ray Data Collection. A tabular crystal, measuring 0.25 × 0.17 × 0.30 mm, was sealed into a glass capillary in air. Data were taken on a Syntex P3 diffractometer. The space group and approximate unit cell dimensions were determined from preliminary scans and rotation photographs. An ω scan from a typical reflection gave a peak width at half-maximum of 0.30°, indicating that the crystal was of satisfactory quality. The cell dimensions were refined from the Bragg angles of 50 computer-centered reflections.

Intensity data were collected in the range 4–55° in 2θ, by using the ω-scan method with a 1° scan range, a variable scan rate of 4–10°/min, and background measurements at both ends of the scan with total background time equal to scan time. The crystal temperature was maintained at –100 °C. A total of 6100 independent reflections were measured. Four standard reflections were monitored at intervals of 200 reflections. No crystal decay was observed. An empirical absorption correction was applied to the raw data, on the basis of a 10° interval ψ scan of a single reflection. Transmission factors were in the range 0.908–0.999.

Solution and Refinement. Data reduction, solution, and refinement of the structure were done on a VAX/VMS V01 DEC computer, using an in-house package of programs supplied by Dr. J. C. Calabrese. Atomic scattering factors were taken from the tabulations of Cromer and Waber.[8a] Anomalous dispersion corrections were from Cromer.[8b] In the full-matrix least-squares refinement, the function minimized was $w|F_o| - |F_c|)^2$, where the weight, w, was taken as $1/\sum(F)$. The standard deviation of the observed structure factor was derived from the counting statistics by using an "ignorance factor",[9] $p = 0.055$. The structure was solved by a version of the MULTAN direct-methods program and by successive Fourier and difference-Fourier electron density maps.

Results

Depending upon rather subtle changes in reaction conditions, the reaction of $MoO_3\cdot2H_2O$ and pyridine results in the formation of either of two polycrystalline pyridinium molybdate phases. Under slightly more vigorous conditions (60 °C, 72
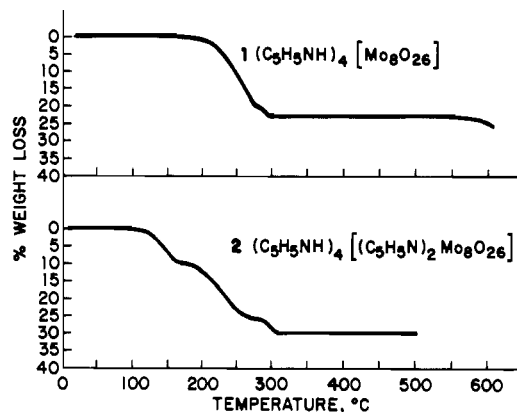

Figure 1. TGA curves (heating rate 5 °C/min in O_2) for the two pyridinium molybdate phases.

Table I. Powder X-Ray Diffraction Patterns

2θ	d, Å	I/I_0	2θ	d, Å	I/I_0
		$(C_5H_5NH)_4[Mo_8O_{26}]$ (1)			
8.33	10.61	60	22.96	3.87	2
8.99	9.83	70	23.93	3.72	30
10.10	8.75	100	25.17	3.54	30
10.91	8.10	2	25.41	3.50	20
13.33	6.64	10	26.84	3.32	30
17.31	5.12	50	27.21	3.27	10
20.51	4.33	2	28.08	3.18	30
22.19	4.00	10	29.40	3.04	2
		$(C_5H_5NH)_4[(C_5H_5N)_2Mo_8O_{26}]$ (2)			
8.53	10.35	10	19.07	4.65	2
8.88	9.95	80	19.84	4.47	5
9.34	9.46	10	20.93	4.24	80
9.78	9.04	70	21.39	4.14	60
10.09	8.76	90	22.29	3.98	50
11.75	7.52	20	23.40	3.80	50
11.92	7.42	40	23.80	3.74	10
12.62	7.01	2	25.37	3.51	40
13.38	6.61	40	26.13	3.41	20
14.62	6.05	40	26.59	3.35	20
15.24	5.81	40	26.96	3.30	5
15.41	5.75	40	27.35	3.26	10
15.94	5.56	5	27.58	3.23	100
16.65	5.32	50	29.89	2.99	10
17.87	4.96	50			

h), the simple octamolybdate $(C_5H_5NH)_4[Mo_8O_{26}]$ (1) is formed. This stoichiometry was confirmed by TGA in oxygen (Figure 1) coupled with mass spectrometry. The thermal decomposition of this phase produces 4 equiv of pyridine/2 equiv of water. The residue, 8 equiv of MoO_3, was identified by X-ray powder diffraction.

Reaction of $MoO_3\cdot2H_2O$ with pyridine under milder conditions (45 °C, 24 h) produces a second pyridinium molybdate phase. A comparison of the powder diffraction patterns for the two phases is given in Table I. A comparison of the TGA curves (Figure 1) of the two molybdates indicated the presence, in the second phase, of an additional 2 equiv of weakly bound pyridine (subsequently confirmed by mass spectrometry). Removal of this extra bound pyridine by heating to 100 °C under vacuum gives the simple molybdate 1. In light of the previous report by Johnson et al.,[6] it seemed plausible to propose that this pyridine-containing molybdate be formulated as $(C_5H_5NH)_4[(C_5H_5N)_2Mo_8O_{26}]$ (2).

Both infrared and Raman spectra were obtained on samples $(C_5H_5NH)_4[Mo_8O_{26}]$ (1) and $(C_5H_5NH)_4[(C_5H_5N)_2Mo_8O_{26}]$ (2). The vibrational modes of pyridine undergo well-characterized shifts dependent upon whether the pyridine is protonated or bound through the nitrogen lone pair.[10] Table II compares the infrared data obtained for samples 1 and 2 with that of $(C_5H_5N)MoO_3$.[6] Sample 1 has bands at 1636, 1613, 1540, and 1484 cm^{-1}. These are characteristic of pyridinium

(8) "International Tables for X-ray Crystallography"; Kynoch Press: Birmingham, England, 1974; Vol. IV: (a) Table 2.2B; (b) Table 2.3.1.
(9) Corfield, P. W. R.; Doedens, R. J.; Ibers, J. A. *Inorg. Chem.* **1967**, *6*, 197.
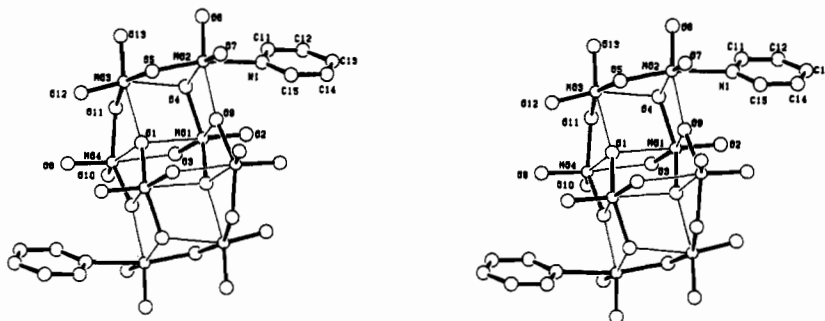
Figure 2. Stereoscopic view of the $[(C_5H_5N)_2Mo_8O_{26}]^{4-}$ anion.[26]

Table II. Comparison of Infrared and Raman Data

$(C_5H_5NH)_4$- $[Mo_8O_{26}]$	$(C_5H_5NH)_4$- $[(C_5H_5N)_2Mo_8O_{26}]$	(C_5H_5N)- MoO_3[6]
	IR Bands	
1636 (m)	1634 (m)	1644 (w)
1613 (vs)	1605 (s)	1603 (s)
	1568 (w)	1572 (m)
1540 (s)	1541 (m)	
	1528 (s)	
1484 (s)	1487 (vs)	1485 (m)
	1448 (s)	1445 (vs)
	Raman Bands	
1485	1482	
	1570	
1612	1608	
1637	1635	

Table III. X-ray Crystallographic Data

formula	$Mo_4O_{14}N_3SC_{17}H_{23}$
fw	909.21
cryst syst	monoclinic
space group	$P2_1/n$
a, Å	11.388 (1)
b, Å	13.761 (2)
c, Å	17.547 (3)
β, deg	100.70 (1)
V, Å^3	2702 (1)
Z	4
ρ(calcd), g cm^{-3}	2.235
radiation (λ, Å)	Mo Kα (0.710 69)
monochromator	graphite
cryst dimens, mm	0.25 × 0.17 × 0.30
no. of reflcns collcd	6101
no. of reflcns used	4937
no. of variables refined	427
R	0.0379
R_w	0.0468

ion.[10] Sample **2** has, in addition to the previously mentioned bands, features at 1568 (weak), 1528, and 1448 cm^{-1}. These additional bands are characteristic of weakly coordinatively bound pyridine[10] and compare favorably with those bands found for $(C_5H_5N)MoO_3$.[6] The Raman data, also listed in Table II, confirm these results, with sample **1** exhibiting bands at 1485, 1612, and 1637 cm^{-1} and sample **2** showing an additional strong band at 1570 cm^{-1}. The features in both the Raman and infrared spectra are consistent with the proposed structure of **2** involving additional weakly bound pyridine molecules.

In order to locate the coordinately bound pyridine, numerous attempts at crystal growth were made. Suitable single crystals for structure determination were obtained by recrystallizing the polycrystalline powder of **2** from a 2:1 mixture, by volume, of dimethyl sulfoxide and pyridine.

(10) Gill, N. S.; Nuttall, R. H.; Scaife, D. E.; Sharp, D. W. A. *J. Inorg. Nucl. Chem.* **1961**, *18*, 79.

Table IV. Atomic Coordinates (×10^4) and Isotropic Thermal Parameters for $(C_5H_5NH)_4[(C_5H_5N)_2Mo_8O_{26}]\cdot2Me_2SO$

atom	x	y	z	B_{iso}, Å^2
Mo(1)	4278.8 (4)	5389.1 (3)	4118.9 (2)	
Mo(2)	6409.9 (4)	4625.4 (3)	3172.0 (3)	
Mo(3)	4996.8 (4)	2942.3 (3)	3921.8 (2)	
Mo(4)	3249.8 (4)	3491.6 (3)	5125.8 (2)	
S	2625 (2)	5193 (1)	−252 (1)	
O(1)	5044 (3)	4019 (2)	4909 (2)	
O(2)	3738 (4)	6357 (3)	3551 (2)	
O(3)	2997 (3)	4880 (3)	4367 (2)	
O(4)	4582 (3)	4437 (2)	3389 (2)	
O(5)	6552 (4)	3539 (3)	3833 (2)	
O(6)	6020 (4)	4103 (3)	2279 (2)	
O(7)	7860 (4)	4983 (3)	3215 (3)	
O(8)	3725 (4)	2473 (3)	5652 (2)	
O(9)	3857 (3)	4445 (2)	5919 (2)	
O(10)	1742 (3)	3506 (3)	5067 (2)	
O(11)	3409 (3)	2986 (3)	4120 (2)	
O(12)	5621 (4)	2060 (3)	4567 (2)	
O(13)	4680 (4)	2366 (3)	3048 (2)	
O(14)	3268 (5)	4645 (3)	442 (3)	
N(1)	5709 (4)	6006 (4)	2527 (3)	
N(2)	3940 (5)	8435 (4)	3659 (3)	
N(3)	1110 (7)	5968 (8)	4772 (6)	
C(1)	3633 (9)	6082 (6)	−485 (5)	
C(2)	2616 (10)	4438 (8)	−1073 (5)	
C(11)	4678 (6)	5977 (5)	2014 (3)	
C(12)	4211 (8)	6791 (7)	1609 (4)	
C(13)	4860 (9)	7633 (7)	1700 (5)	
C(14)	5912 (9)	7675 (6)	2225 (5)	
C(15)	6317 (6)	6838 (5)	2638 (4)	
C(21)	4452 (6)	9254 (5)	3949 (4)	
C(22)	4211 (7)	10107 (5)	3567 (5)	
C(23)	3438 (8)	10104 (6)	2858 (5)	
C(24)	2904 (10)	9260 (7)	2593 (6)	
C(25)	3175 (8)	8426 (5)	2989 (5)	
C(31)	1621 (8)	6795 (13)	4900 (6)	
C(32)	1291 (12)	7575 (9)	4400 (6)	
C(33)	563 (8)	7442 (6)	3746 (5)	
C(34)	83 (6)	6551 (6)	3579 (4)	
C(35)	352 (8)	5820 (8)	4092 (5)	
H(1A)	3604 (101)	6767 (85)	−232 (66)	8.5 (30)
H(1B)	4295 (58)	5790 (47)	−232 (66)	8.5 (30)
H(1C)	3312 (69)	6273 (58)	−970 (49)	4.1 (18)
H(2A)	3373 (59)	4165 (43)	−1047 (34)	4.5 (27)
H(2B)	2451 (60)	4901 (50)	−1480 (40)	4.0 (19)
H(2C)	2229 (87)	4134 (71)	−1010 (57)	4.5 (27)
H(11)	4257 (45)	5341 (38)	2011 (28)	0.5 (9)
H(12)	3514 (58)	6769 (46)	1245 (37)	2.1 (13)
H(13)	4547 (79)	8320 (67)	1533 (50)	5.7 (22)
H(14)	6188 (71)	8262 (60)	2308 (45)	4.1 (19)
H(15)	7043 (70)	6868 (60)	3005 (50)	2.0 (13)
H(21)	5065 (72)	9125 (61)	4590 (48)	5.1 (20)
H(22)	4559 (70)	10571 (61)	3725 (46)	3.9 (18)
H(23)	3148 (77)	10607 (65)	2654 (51)	5.0 (21)
H(24)	2661 (84)	9259 (71)	2236 (52)	3.8 (24)
H(25)	2940 (73)	7844 (59)	2821 (45)	4.2 (18)
H(31)	1662 (116)	7107 (100)	5110 (71)	4.3 (41)
H(32)	1270 (71)	7898 (51)	4461 (46)	−1.2 (18)
H(33)	540 (93)	7827 (70)	3572 (58)	4.0 (27)
H(34)	−367 (102)	6371 (85)	3162 (65)	8.6 (32)
H(35)	−160 (80)	5161 (72)	4011 (53)	5.9 (23)

Table V. Selected Atomic Distances (Å) for $[(C_5H_5N)_2Mo_8O_{26}]^{4-}$

Mo(1)–O(1)	1.918 (3)	Mo(3)–O(1)	2.272 (3)
Mo(1)–O(1)	2.406 (3)	Mo(3)–O(4)	2.272 (3)
Mo(1)–O(2)	1.709 (4)	Mo(3)–O(5)	1.984 (4)
Mo(1)–O(3)	1.746 (4)	Mo(3)–O(11)	1.904 (4)
Mo(1)–O(4)	1.908 (4)	Mo(3)–O(12)	1.721 (4)
Mo(1)–O(9)	2.149 (4)	Mo(3)–O(13)	1.705 (4)
Mo(2)–O(4)	2.200 (4)	Mo(4)–O(1)	2.267 (3)
Mo(2)–O(5)	1.881 (4)	Mo(4)–O(3)	2.316 (4)
Mo(2)–O(6)	1.707 (4)	Mo(4)–O(8)	1.711 (4)
Mo(2)–O(7)	1.711 (4)	Mo(4)–O(9)	1.943 (3)
Mo(2)–O(9)	2.111 (3)	Mo(4)–O(10)	1.701 (4)
Mo(2)–N(1)	2.279 (5)	Mo(4)–O(11)	1.937 (3)
C(11)–C(12)	1.379 (10)	C(11)–H(11)	0.998 (51)
C(12)–C(13)	1.368 (13)	C(12)–H(12)	0.922 (64)
C(13)–C(14)	1.370 (12)	C(13)–H(13)	1.034 (91)
C(14)–C(15)	1.392 (10)	C(14)–H(14)	0.870 (80)
C(11)–N(1)	1.340 (8)	C(15)–H(15)	0.987 (56)
C(15)–N(1)	1.334 (8)		

Table VI. Selected Bond Angles (deg) for $[(C_5H_5N)_2Mo_8O_{26}]^{4-}$

O(1)–Mo(1)–O(1)	77.2 (1)	O(1)–Mo(3)–O(4)	72.4 (1)
O(1)'–Mo(1)–O(2)	103.3 (2)	O(1)–Mo(3)–O(5)	84.0 (1)
O(1)–Mo(1)–O(2)	179.5 (8)	O(1)–Mo(3)–O(11)	74.3 (1)
O(1)'–Mo(1)–O(3)	99.5 (2)	O(1)–Mo(3)–O(12)	90.6 (2)
O(1)–Mo(1)–O(3)	76.8 (1)	O(1)–Mo(3)–O(13)	163.8 (2)
O(1)'–Mo(1)–O(4)	142.7 (1)	O(4)–Mo(3)–O(5)	73.4 (1)
O(1)–Mo(1)–O(4)	75.9 (1)	O(4)–Mo(3)–O(11)	85.1 (1)
O(1)'–Mo(1)–O(9)	75.3 (1)	O(4)–Mo(3)–O(12)	159.7 (2)
O(1)–Mo(1)–O(9)	81.2 (1)	O(4)–Mo(3)–O(13)	93.3 (2)
O(2)–Mo(1)–O(3)	103.4 (2)	O(5)–Mo(3)–O(11)	153.3 (1)
O(2)–Mo(1)–O(4)	103.6 (2)	O(5)–Mo(3)–O(12)	94.5 (2)
O(2)–Mo(1)–O(9)	98.6 (2)	O(5)–Mo(3)–O(13)	99.5 (2)
O(3)–Mo(1)–O(4)	99.0 (2)	O(11)–Mo(3)–O(12)	101.1 (2)
O(3)–Mo(1)–O(9)	158.0 (1)	O(11)–Mo(3)–O(13)	97.4 (2)
O(4)–Mo(1)–O(9)	75.5 (1)	O(12)–Mo(3)–O(13)	104.8 (2)
O(4)–Mo(2)–O(5)	77.0 (2)	O(1)–Mo(4)–O(3)	70.1 (1)
O(4)–Mo(2)–O(6)	90.9 (2)	O(1)–Mo(4)–O(8)	98.5 (2)
O(4)–Mo(2)–O(7)	164.3 (2)	O(1)–Mo(4)–O(9)	72.1 (1)
O(4)–Mo(2)–O(9)	70.6 (1)	O(1)–Mo(4)–O(10)	156.6 (2)
O(5)–Mo(2)–O(6)	102.1 (2)	O(1)–Mo(4)–O(11)	73.9 (1)
O(5)–Mo(2)–O(7)	103.3 (2)	O(3)–Mo(4)–O(8)	168.4 (2)
O(5)–Mo(2)–O(9)	91.4 (2)	O(3)–Mo(4)–O(9)	81.0 (1)
O(6)–Mo(2)–O(7)	104.3 (2)	O(3)–Mo(4)–O(10)	86.5 (2)
O(6)–Mo(2)–O(9)	154.2 (2)	O(3)–Mo(4)–O(11)	78.2 (1)
O(7)–Mo(2)–O(9)	93.7 (2)	O(8)–Mo(4)–O(9)	97.6 (2)
O(4)–Mo(2)–N(1)	85.9 (2)	O(8)–Mo(4)–O(10)	104.9 (2)
O(5)–Mo(2)–N(1)	162.0 (2)	O(8)–Mo(4)–O(11)	97.1 (2)
O(6)–Mo(2)–N(1)	83.5 (2)	O(9)–Mo(4)–O(10)	104.8 (2)
O(7)–Mo(2)–N(1)	91.6 (2)	O(9)–Mo(4)–O(11)	144.5 (1)
O(9)'–Mo(2)–N(1)	77.5 (1)	O(10)–Mo(4)–O(11)	102.3 (2)

The structure solution did indeed confirm that the octamolybdate anion contains coordinately bound pyridine as shown in Figure 2. The crystallographic parameters, atomic coordinates, bond distances, and bond angles are displayed in Tables III–VI, respectively.

Discussion

The enhanced reactivity of $MoO_3 \cdot 2H_2O$ relative to MoO_3 at low temperature has been demonstrated recently.[1,4,11] Presumably, this is a consequence of the ease at which an open coordination site (marked by an asterisk) can be produced by loss of the base, H_2O, at the octahedral molybdenum site:
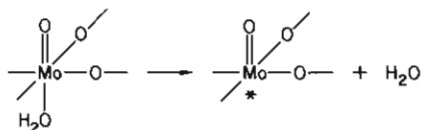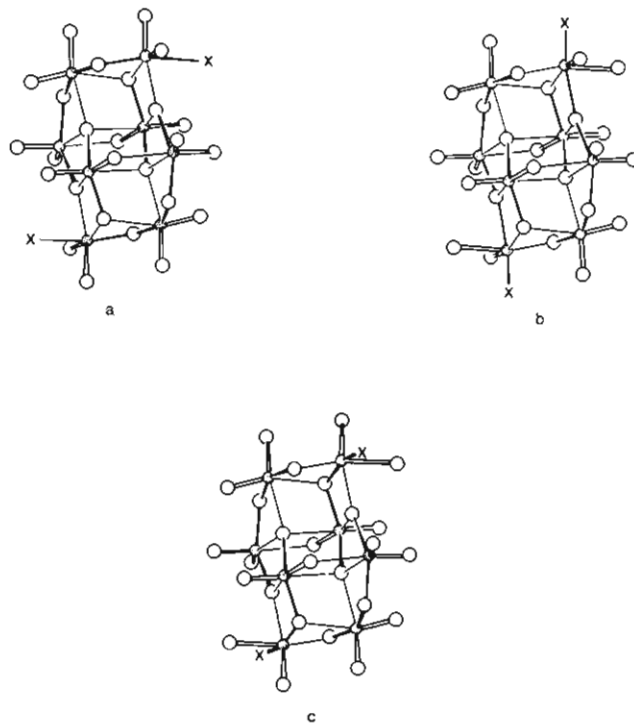
Figure 3. Linkage isomers of $[(X)_2Mo_8O_{26}]^{2n-4}$. Short molybdenum to oxygen bonds are indicated by double lines, intermediate bonds by bold single lines, and long bonds by thin lines. The molybdenum atoms are shaded. For a, X = C_5H_5N, HO, HCOO, and $[Mo_8O_{26}O_{2/2}]_n$; for b, X = CH_3O and MoO_4.

In the $MoO_3/H_2O/Me_2SO$ system[11] simple base substitution has been observed. In the $MoO_3/H_2O/C_5H_5N$ system, not only does base substitution occur, but also the liberated water produces a hydrolysis to molybdate:

$$8MoO_3 \cdot 2H_2O + 6C_5H_5N \rightarrow$$
$$(C_5H_5NH)_4[(C_5H_5N)_2Mo_8O_{26}] + 14H_2O$$
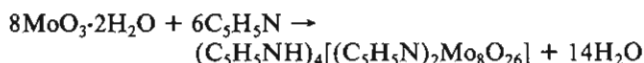
Under more vigorous conditions, the coordinated C_5H_5N is lost, leaving the simple molybdate $(C_5H_5NH)_4[Mo_8O_{26}]$.[12]

$[(C_5H_5N)_2Mo_8O_{26}]^{4-}$ represents the first example of a non-oxygen-bound ligand coordinated directly to a molybdenum atom of an isopolymolybdate anion. The structure of $[(C_5H_5N)_2Mo_8O_{26}]^{4-}$ is analogous to a number of other octamolybdate anions: $[H_2Mo_8O_{28}]^{6-}$[13] $\equiv [(HO)_2Mo_8O_{26}]^{6-}$; $[(HCO)_2Mo_8O_{28}]^{6-}$[2] $\equiv [(HCOO)_2Mo_8O_{26}]^{6-}$; and the condensation polymer of the octamolybdate itself, $[Mo_8O_{27}]_n^{6-}$[14] $\equiv [O_{2/2}Mo_8O_{26}]_n^{6-}$. On the basis of the formulation $[(C_5H_5N)_2Mo_8O_{26}]^{4-}$, a general description of these octamolybdates would be $[(X)_2Mo_8O_{26}]^{(2n-4)}$, where n is the formal charge of the coordinated base, X. The framework of the octamolybdate anion common to the above mentioned anions is shown in Figure 3a. Note that each molybdenum atom in this structure (Figure 3; Table V) exhibits the typical 2 + 2 + 2 distorted octahedral coordination observed in both iso- and heteropolymolybdates and also numerous molybdenum(VI) oxide systems.[5]

It is also interesting to note that while having the same general structural elements as $[(C_5H_5N)_2Mo_8O_{26}]^{4-}$ and the other octamolybdates cited above, the anions $[Mo_{10}O_{34}]^{8-}$[15]

(11) McCarron, E. M., III; Harlow, R. L. *J. Chem. Soc., Chem. Commun.* **1983**, 90.

(12) Schwing-Weill, M.-J. *Bull. Soc. Chim. Fr.* **1969**, 1481. Arnaud-Nue, F; Schwing-Weill, M.-J. "Proceedings of the Climax 1st International Conference on the Chemistry and Uses of Molybdenum"; Mitchell, P. C. H., Ed.; Climax Molybdenum Co.: Ann Arbor, MI, 1982.

(13) Isobe, M.; Marumo, F.; Yamase, T.; Ikawa, T. *Acta Crystallogr. Sect. B: Struct. Crystallogr. Cryst. Chem.* **1978**, *B34*, 2728.

(14) Boschen, I.; Buss, B.; Krebs, B. *Acta Crystallogr. Sect. B: Struct. Crystallogr. Cryst. Chem.* **1974**, *B30*, 48.

Table VII. Interaction Parameters for the Mo–X Bond of the Anions $[(X)_2Mo_xO_{26}]^{2n-4}$

X	ref	formal charge	approx steric vol, A^3	bond length, A	bond strength	conformn[f]
C_5H_5N	a	0	135[b]	2.279	0.32	a
HCOO	2	1–	60[b]	2.105	0.51	a
HO	13	1–	20[c]	1.972	0.76	a
$Mo_xO_{26}O_{2/2}$	14	6–	50[d]	1.889	0.98	a
MoO_4	18	2–	65[e]	1.978	0.74	b
CH_3O	1	1–	65[c]	1.907	0.92	b

[a] This work. [b] Calculated from liquid density for NC_5H_5 and HCOOH. [c] From: Ucvloop, A; et al. "Drug Design"; Ariens, E. J., Ed.; Academic Press: New York, 1976, p 165. [d] Average structural volume for the MoO_6 octahedron (calculated for MoO_3). [e] Average structural volume for the MoO_4 tetrahedron (calculated for A_2MoO_4). [f] From Figure 3.

Table VIII. Corresponding Bond Lengths (d, A) and Bond Strengths (s) for the $XMoO_5$ Octahedron of the Octamolybdates $[(X)_2Mo_8O_{26}]^{2n-4}$

	X							
	C_5H_5N[a]		$O_{2/2}Mo_8O_{26}$[14]		OH[13]		OCHO[2]	
	d	s	d	s	d	s	d	s
Mo–O(1)	1.711	1.77	1.714	1.75	1.709	1.78	1.703	1.82
–O(2)	2.200	0.39	2.198	0.39	2.308	0.29	2.234	0.36
–O(3)	1.707	1.80	1.716	1.74	1.722	1.70	1.707	1.80
–O(4)	2.111	0.50	2.196	0.40	2.138	0.47	2.172	0.42
–O(5)	1.881	1.00	2.046	0.61	1.975	0.75	1.917	0.90
–X	2.279	0.32	1.889	0.98	1.972	0.76	2.105	0.51
BO = $\Sigma(s)$[b]		5.78		5.87		5.75		5.80

[a] This work. [b] Bond order (BO) of molybdenum is equal to the sum of the bond strengths (see ref 16).

$\equiv [(MoO_4)_2Mo_8O_{26}]^{8-}$ and $[Mo_8O_{24}(OCH_3)_4]^{4-1}$ $\equiv [(CH_3O)_2Mo_8O_{24}(\mu\text{-}OCH_3)_2]$ adopt a different mode of linkage, as shown in Figure 3b. Table VII lists the sizes and formal charges of the bases, X, for the known $[(X)_2Mo_8O_{26}]^{(2n-4)}$ anions. On the basis of these Table VII values, there appears to be neither a clear steric nor electronic reason for this linkage isomerism and, therefore, crystal-packing forces presumably determine which structure is adopted.

Although structurally similar, $[(C_5H_5N)_2Mo_8O_{26}]^{4-}$ is distinguished from the other octamolybdates containing oxygen-bound groups, $[(RO)_2Mo_8O_{26}]^{(2n-4)}$ (where n is the formal charge of the group RO), by the difference in the strength of the Mo–N vs. the Mo–OR interaction. The relative strength of these interactions is reflected in the bond lengths given in Table VII for the various anions. The bond strengths, s, are derived from the expression[16]

$$s = (d/1.882)^{-6.0}$$

where d is the bond length in Å. For the oxygen-bound groups

Table IX. Molybdenum Trioxide/Free Base Interactions

	ref	d, A	s	dissociation temp,[a] °C
$MoO_3 \cdot dien$[b]	24	2.324	0.28	
$MoO_3 \cdot 2H_2O$	25	2.293	0.31	~120
$Mo_3O_9 \cdot 4Me_2SO$	11	2.245	0.35	~180
$(C_5H_5N)MoO_3$	6			~215
$[(C_5H_5N)_2Mo_8O_{26}]^{4-}$	c	2.279	0.32	~150

[a] In O_2, heating rate 5 °C/min. [b] dien = diethylenetriamine. [c] This work.
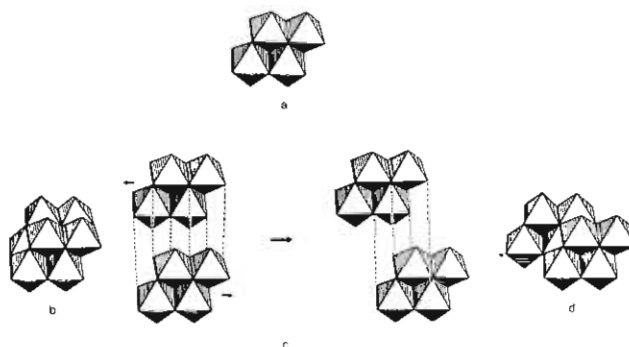
Figure 4. Relationship between β-$[Mo8O_{26}]^{4-}$ and $[(*)_2Mo_8O_{26}]^{4-}$ viewed as resulting from a shearing of $[Mo_4O_{13}]^{2-}$ asymmetric units (a) of β-$[Mo_8O_{26}]^{4-}$ (b) parallel to one another (separated for clarity only) (c), to produce the open coordination sites denoted by asterisks shown in d.

that all carry formal negative charge, the Mo–O bond orders range from roughly $^1/_2$ to 1, depending upon the amount of negative charge concentrated at the oxygen atom.[17] On the other hand, the interaction between molybdenum and the neutral base, pyridine, is much weaker, having a bond order of $\sim^1/_3$ and reflecting the absence of a strong electrostatic component to the bonding. As a consequence of this weak Mo–N bond,[18] the Mo–O bonds that complete the distorted octahedron about Mo(2) (Figure 2) compensationally strengthen, as can be seen by comparing the corresponding bond lengths for the structures, $[(X)_2Mo_8O_{26}]^{2n-4}$ listed in Table VIII. This low Mo–N bond strength is consistent with the bond strengths observed for other interactions between molybdenum(VI) and neutral base ligands. Table IX lists bond strengths and dissociation temperatures for known molybdenum trioxide/free base interactions. For this type of interaction a bond strength of $\sim^1/_4$ to $^1/_3$ is fairly typical. Unfortunately, a direct comparison of the bonding in $[(C_5H_5N)_2Mo_8O_{26}]^{4-}$ and $(C_5H_5N)MoO_3$ is not possible since the structure of $(C_5H_5N)MoO_3$ is not known in detail.[6] But, on the basis of the thermal dissociation temperatures, it appears that the pyridine of $(C_5H_5N)MoO_3$ is more strongly bound than the pyridine in $[(C_5H_5N)_2Mo_8O_{26}]^{4-}$ (although this may simply reflect an enhanced hydrogen-bonding capacity for the layered $(C_5H_5N)MoO_3$).

The relationship between the $[(X)_2Mo_8O_{26}]^{(2n-4)}$ species and β-$[Mo_8O_{26}]^{4-19}$ is illustrated in Figure 4, which shows how a simple shearing of the $(Mo_4O_{13})^{2-}$ asymmetric units of the

(15) Fuchs, J.; Hartl, H.; Hunnius, W.-D.; Mahjour, S. *Angew. Chem., Int. Ed. Engl.* **1975**, *14*, 644.

(16) Bart, J. C. J.; Ragaini, V. "Proceedings of the Climax 3rd International Conference on the Chemistry and Uses of Molybdenum"; Barry, H. F., Mitchell, P. C. H., Eds.; Climax Molybdenum Co.: Ann Arbor, MI, 1979.

(17) A correlation between the charge density at the oxygen atom and the strength of the Mo–OR bond will be the subject of a subsequent paper describing a new octamolybdate structure.

(18) Generally, the bond between pyridine and molybdenum is weak regardless of molybdenum oxidation state. Mo–N interactions range from 2.2 to 2.5 Å. See: Chisholm, M. H. "Inorganic Chemistry: Toward the 21st Century"; Chisholm, M. H., Ed.; American Chemical Society: Washington, DC, 1983; ACS Symp. Ser. No. 211. Cotton, et al. *J. Am. Chem. Soc.* **1972**, *94*, 5697. Brisdon, et al. *J. Chem. Soc., Dalton Trans.* **1978**, 291. Cotton, et al. *Inorg. Chim. Acta* **1982**, *59*, 213. Schrauzer, et al. *Organometallics* **1982**, *1*, 44.

(19) (a) Lindquist, I. *Ark kemi* **1950**, *2*, 349. (b) Atovmyan, L. O.; Krasochka, O. N. *J. Struct. Chem. (Engl. Transl.)* **1972**, *13*, 319.
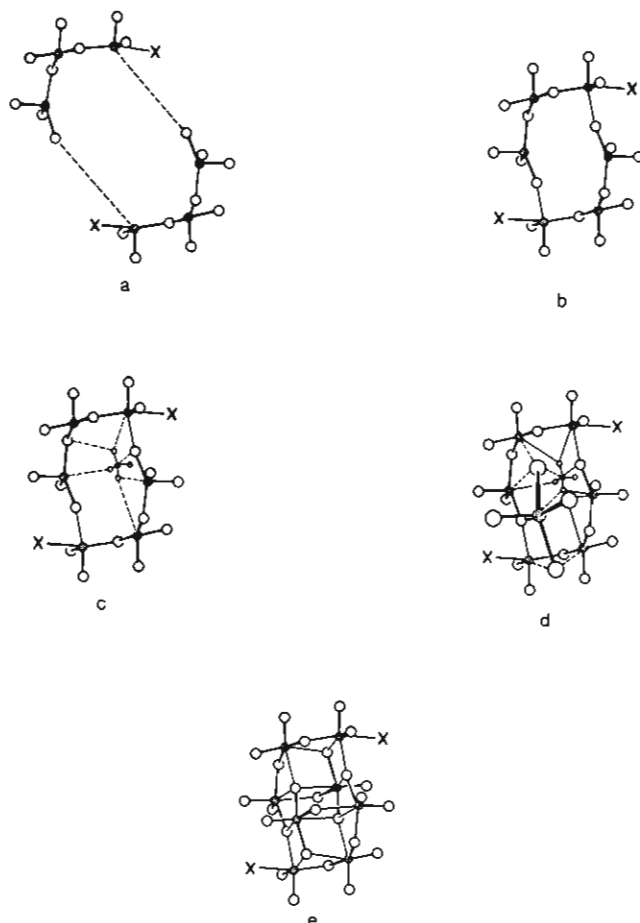
Figure 5. Formation of $[(X)_2Mo_8O_{26}]^{2n-4}$ seen as a condensation of two $[XMo_3O_9]^n$ units (a) to form a hexameric ring (b) that is subsequently approached from below (c) and above (d) by MoO_4^{2-} anions to complete the structure (e). The dashed interactions equate with weak bonds in the structure. The molybdenum atoms are shaded.

parent β-$[Mo_8O_{26}]^{4-}$ anion parallel to one another can produce the observed stoichiometry

$$[Mo_8O_{26}]^{4-} \rightarrow [(*)_2Mo_8O_{26}]^{4-}$$

$$[(*)_2Mo_8O_{26}]^{4-} + 2X^n \rightarrow [(X)_2Mo_8O_{26}]^{(2n-4)}$$
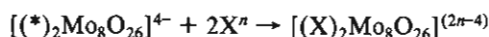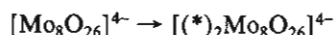
While it is appealing in its simplicity, this scheme fails as a mechanism since it would require the breaking of an inordinate number of bonds and would lead to yet a third linkage isomer (shown in Figure 3c), an example of which has not been observed.

A more plausible mechanism[20] for the formation of these coordinated octamolybdates can be envisioned if one focuses

on bond length alternation (Figure 3; Table V). If one assumes that the long Mo–O bonds result from a condensation-induced distortion of tetrahedrally bonded fragments toward octahedral coordination, then it appears that $[(X)_2Mo_8O_{26}]^{(2n-4)}$ is the product of a condensation of two $[XMo_3O_9]^n$ tetrahedral chains to form a six-membered ring, which then interacts with two MoO_4^{2-} groups as shown in Figure 5. This mechanism would account for the observed linkage isomerism of structures in Figure 3a, b.[21] On the other hand, the isomer in Figure 3c would necessitate the condensation of two tetrhedral $[XMo_2O_6]^n$ dimers and two $[Mo_2O_7]^{2-}$ groups. That the isomer in Figure 3c has not been observed implies that it most likely represents a higher energy structure relative to that derived from MoO_4^{2-} anions and $[XMo_3O_9]^n$ tetrahedral chains.[22] In support of this proposed mechanism, it will be noted that tetrahedral chains of molybdenum oxide exist in the gas phase[23] and, recently, facile octahedral/tetrahedral molybdenum site interconversion has been demonstrated in the MoO_3/Me_2SO system.[11] In fact, the condensation of tetrahedral chains of stoichiometry MoO_3
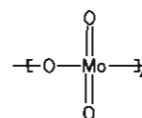
provides an alternate view of the MoO_3 structure.[5]

Conclusion

The structure of $(C_5H_5NH)_4[(C_5H_5N)_2Mo_8O_{26}]\cdot 2Me_2SO$ has been solved. The bonding between the base, pyridine, and molybdenum is found to be weak. As such, $[(C_5H_5N)_2Mo_8O_{26}]^{4-}$ may afford a pathway to many new isopolymolybdates containing organic fragments via substitution reactions, much in the same way that the enhanced reactivity of $MoO_3\cdot 2H_2O$ relative to MoO_3 has expanded molybdenum(VI) oxide chemistry.

(20) This mechanism is an extension of the formation mechanism for isopolymolybdates and -tungstates proposed by: Tytko, K.-H.; Glemser, O. *Adv. Inorg. Chem. Radiochem.* **1976**, *19*, 239. See also: Pope, M. T. "Heteopoly and Isopoly Oxometalates"; Springer-Verlag: New York, 1983; pp 136–141.

(21) This mechanism would also account for the structure of $[Mo_8O_{24}$-$(OCH_3)_4]^{4-}$,[1] which would then be seen as resulting from the condensation of two $[CH_3O-MoO_2-O-MoO_2-O-MoO_2-OCH_3]$ groups and two MoO_4^{2-} anions.

(22) $Mo_2O_7^{2-}$ can in fact be stabilized by utilizing the proper counterion; see: Day, V. W.; Frederick, M. F.; Klemperer, W. G.; Shum, W. *J. Am. Chem. Soc.* **1977**, *99*, 6146. Perhaps with the appropriate selection of counterion, the isomer in Figure 3c may yet be isolated.

(23) Berkowitz, J.; Inghram, M. G.; Chupka, W. A. *J. Chem. Phys.* **1957**, *26*, 842.

(24) Cotton, F. A.; Elder, R. C. *Inorg. Chem.* **1964**, *3*, 397.

(25) Krebs, B. *Acta Crystallogr., Sect. B: Struct. Crystallogr. Cryst. Chem.* **1972**, *B28*, 2222.

(26) ORTEP figure drawn by using arbitrary isotropic temperature factors for the atoms (B_{iso} = 2.0 Å² for Mo, 2.5 Å² for O, N, and C): Johnson, C. K. "ORTEP", Report ORNL-5138; Oak Ridge National Laboratory: Oak Ridge, TN, 1976.